

# Second order quantum renormalisation group of $XXZ$ chain with next nearest neighbour interactions

R. Jafari<sup>1</sup> and A. Langari<sup>1,2</sup> \*

<sup>1</sup>*Institute for Advanced Studies in Basic Sciences, 45195-1159, Zanjan, Iran*

<sup>2</sup>*Max-Planck-Institut für Chemische Physik fester Stoffe, 01187 Dresden, Germany*

(Dated: June 24, 2018)

We have extended the application of quantum renormalisation group (QRG) to the anisotropic Heisenberg model with next-nearest neighbour (n-n-n) interaction. The second order correction has to be taken into account to get a self similar renormalized Hamiltonian in the presence of n-n-n-interaction. We have obtained the phase diagram of this model which consists of three different phases, i.e, spin-fluid, dimerised and Néel types which merge at the tri-critical point. The anisotropy of the n-n-n-term changes the phase diagram significantly. It has a dominant role in the Néel-dimer phase boundary. The staggered magnetisation as an order parameter defines the border between fluid-Néel and Néel-dimer phases. The improvement of the second order RG corrections on the ground state energy of the Heisenberg model is presented. Moreover, the application of second order QRG on the spin lattice model has been discussed generally. Our scheme shows that higher order corrections lead to an effective Hamiltonian with infinite range of interactions.

PACS numbers: 75.10.Jm, 75.10.Pq, 75.40.Cx

*Keywords: Quantum renormalization group, Spin chains, Heisenberg model, Quantum phase transitions, Phase diagram, Second order corrections*

## I. INTRODUCTION

Quantum phase transition has been one of the most interesting topics in the area of strongly correlated systems in the last decade. It is a phase transition at zero temperature where the quantum fluctuations play the dominant role [1]. Suppression of the thermal fluctuations at zero temperature introduces the ground state as the representative of the system. The properties of the ground state may be changed drastically shown as a non-analytic behaviour of a physical quantity by reaching the quantum critical point. This can be done by tuning a parameter in the Hamiltonian, for instance the magnetic field or the amount of disorder. The study of the ground state and its energy is thus of central importance for understanding the critical behaviour of such systems.

The technique of renormalisation group (RG) has been so devised to deal with these multi-scale problems [2, 3, 4]. In the momentum space RG which is suitable for studying the continuous systems, one iteratively integrates out small scale fluctuations and renormalizes the Hamiltonian. In the real space RG, which is usually performed on the lattice systems with discrete variables (i.e quantum spin chain), an original Hamiltonian is replaced with an effective one for a lower energy subspace iteratively. In this approach the Hamiltonian is divided into inter-block ( $H^{BB}$ ) and intra-block parts ( $H^B$ ),  $H^B$  is diagonalized exactly and then  $H^{BB}$  is projected into the low energy subspace of  $H^B$  [5]. The accuracy of this method is determined by the number of states kept in the  $H^B$  subspace and the approach to consider the effect of neglected subspace. The Ising model in a transverse field [6] and the anisotropic Heisenberg model [7] have been studied by quantum renormalisation group (QRG) approach which gives the correct phase diagram. Moreover, the recent study on a more general model,  $XYZ$  in a transverse field, supports the power of this method to study the collective behaviour of the spin models [8].

In this paper we are going to study the effect of higher order corrections on the QRG scheme. In this respect we will consider the one dimensional  $S = \frac{1}{2}$  antiferromagnetic  $XXZ$  chain with next-nearest neighbour (n-n-n) interactions. Because, even in the case of nearest neighbour Heisenberg model the n-n-n interaction will be generated for the renormalized Hamiltonian if we add the second order corrections. Moreover, we will obtain the phase diagram of this model which is a function of the anisotropies and the n-n-n interactions. We have calculated the effective Hamiltonian up to second order in  $H^{BB}$ . The second order correction improves the accuracy of the results. However, it must be taken into account to get a self similar Hamiltonian after each step of QRG for the n-n-n  $XXZ$  chain. In this approach we have considered the effect of the whole states of the block Hamiltonian which are partially ignored in

---

\* Corresponding author: A. Langari, Institute for Advanced Studies in Basic Sciences, P. O. Box. 45195-1159, Zanjan, Iran. e-mail: langari@cpfs.mpg.de,

the first order approach. The present scheme allows us to have the analytic RG equations, which gives a better understanding of the behaviour of system by running of the coupling constants. We have succeeded to obtain the phase diagram which contains the critical surface between the spin-fluid, Néel and dimer phases. The boundaries between these phases merge at the tri-critical point. The projection of our phase diagram on the  $\Delta = \delta$  plane (the same anisotropy for nearest and next-nearest neighbour interactions) is in good agreement with the numerical ones [9]. The QRG equations show that the anisotropy in the n-n-n term changes the phase boundaries significantly. We have also derived the staggered magnetisation in the z direction, that is the proper order parameter to show the phase transition between Néel-dimer and fluid-Néel phases.

In the recent years, several interesting quasi-one-dimensional magnetic systems have been studied experimentally [10, 11, 12]. Among them, some compounds containing  $CuO$  chains with edge-sharing  $CuO_4$  plaquette were expected to be described by the  $XXZ$  model with next-nearest neighbour interaction [13]. The Hamiltonian of this model on a periodic chain of  $N$  sites is:

$$H = \frac{J}{4} \left\{ \sum_{i=1}^N [\sigma_i^x \sigma_{i+1}^x + \sigma_i^y \sigma_{i+1}^y + \Delta \sigma_i^z \sigma_{i+1}^z + J_2 (\sigma_i^x \sigma_{i+2}^x + \sigma_i^y \sigma_{i+2}^y + \delta \sigma_i^z \sigma_{i+2}^z)] \right\}, \quad (1)$$

where  $J > 0$  and  $J \times J_2 \geq 0$  are the first and second-nearest neighbour exchange couplings and the corresponding easy-axis anisotropies are defined by  $\Delta$  and  $\delta$ . For  $J_2 = 0$ , the ground state properties are well known by the Bethe ansatz [14] and the bosonization technique. In this case, for  $\Delta < -1$ , the system is in the ferromagnetic phase, while for  $\Delta > 1$ , it enters the Néel phase where the twofold degenerate ground states are separated from the excited ones by a finite gap [15]. In the case of  $XY$ -type anisotropy ( $-1 \leq \Delta \leq 1$ ) quantum fluctuations destroy the long range order even at the zero temperature. The ground state is characterised by gapless excitations and algebraic decay of spin correlations (spin-fluid). A kind of frustration can be introduced to this model by adding the next-nearest neighbour interaction ( $J_2 \neq 0$ ) as well as the nearest neighbour ones. On the  $J_2 = \frac{1}{2}, \Delta = \delta = 1$  line, the model is known as the Majumdar-Ghosh Hamiltonian where the exact ground state has been obtained to be purely dimerised [16]. The dimer state is characterised by the excitation gap, the exponential decay of the spin correlation functions and the dimer long-range order. According to the above facts, there should exist the fluid, dimer and Néel phases in this model. The isotropic model have been studied intensively by analytic and numerical approaches [16]–[26]. However, the QRG approach to this model has not been considered yet which gives a clear phase diagram in the presence of anisotropies. Moreover, as mentioned earlier, we are going to address the implementation of higher order RG corrections and discuss its features. We will explain the QRG scheme in the next section where the second order effective Hamiltonian and the renormalisation of the coupling constants are obtained. In Sec. III, We will present the phase diagram and explain the border between different phases. Finally, we will discuss on the features of the second order approach and higher order corrections.

## II. RG EQUATIONS

The main idea of the RG method is the mode elimination or thinning of the degrees of freedom followed by an iteration which reduces the number of variables step by step until reaching a fixed point. We have implemented the Kadanoff's block method for this purpose, because they are well suited to perform analytical calculations in the lattice models and they are conceptually easy to be extended to the higher dimensions. In Kadanoff's method, the lattice is divided into  $N'$  blocks with  $n_s$  sites each and the original non-diagonal Hamiltonian is replaced with an effective one for a lower energy subspace. The Hamiltonian can be written

$$H = H^B + \lambda H^{BB}, \quad (2)$$

where the block Hamiltonian  $H^B$  is a sum of commuting Hamiltonians, each acting on every block and  $\lambda$  is a coupling constant which is already in  $H$  or else it can be introduced as a parameter characterising the inter-block coupling which can be set to 1 at the end of calculation. An exact implementation of this method [5] is given by the following equation,

$$H^{eff} = P_B H P_B, \quad (3)$$

where  $P_B$  is the projection operator. Eq.(2) suggests that we should search for the solution of the Eq.(3) in the form of a perturbative expansion in the inter-block coupling parameter  $\lambda$ , namely

$$P_B = P_0 + \lambda P_1 + \lambda^2 P_2 + \dots, \quad H^{eff} = H_0^{eff} + \lambda H_1^{eff} + \lambda^2 H_2^{eff} + \dots. \quad (4)$$

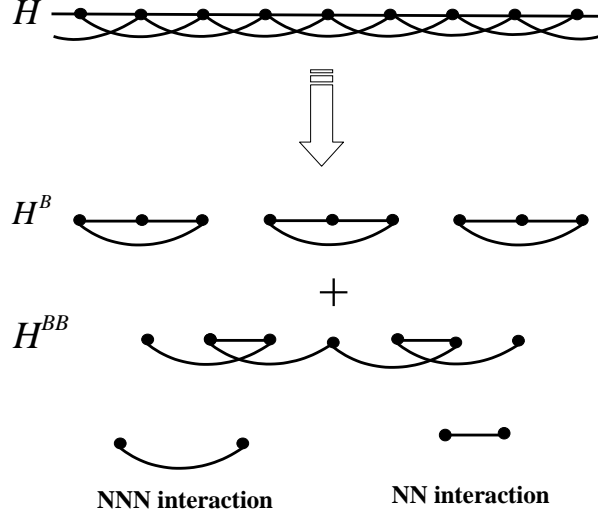


FIG. 1: The decomposition of chain into the three site blocks Hamiltonian ( $H^B$ ) and the inter-block Hamiltonian ( $H^{BB}$ ).

To the zeroth order in  $\lambda$  Eq.(3) becomes

$$H_0^{eff} = P_0 H^B P_0. \quad (5)$$

Since  $H^B$  is a sum of disconnected block Hamiltonians

$$H^B = \sum_{I=1}^{N'} h_I^B,$$

one can search for a solution of  $P_0$  in a factorised form

$$P_0 = \prod_{I=1}^{N'} P_0^I.$$

It can be found that

$$P_0^I = \sum_{i=1}^k |\psi_i\rangle \langle \psi_i|,$$

where  $|\psi_i\rangle$  ( $i = 1, \dots, k$ ) are the  $k$  lowest energy states of  $h_I^B$ . First and second order corrections are obtained to be

$$H_1^{eff} = P_0 H^{BB} P_0, \quad H_2^{eff} = P_0 H^{BB} P_1, \quad (6)$$

where  $P_1$  is defined by the following equation

$$P_1 = (1 - P_0) \frac{1}{E_0 - H^B} (1 - P_0) H^{BB} P_0.$$

The second order correction can be written[27, 28],

$$H_2^{eff} = P_0 [H^{BB} (1 - P_0) \frac{1}{E_0 - H^B} (1 - P_0) H^{BB}] P_0. \quad (7)$$

We have considered three-site block (Fig.(1)) and kept the degenerate ground states ( $|\psi_0\rangle, |\psi'_0\rangle$ ) of each block to construct the projection operator ( $P_0 = |\psi_0\rangle\langle\psi_0| + |\psi'_0\rangle\langle\psi'_0|$ ). The ground states and their corresponding eigenvalues of each block are

$$\begin{aligned} |\psi_0\rangle &= \frac{1}{\sqrt{2+q^2}}(|\uparrow\uparrow\downarrow\rangle + q|\uparrow\downarrow\uparrow\rangle + |\downarrow\uparrow\uparrow\rangle), \\ |\psi'_0\rangle &= \frac{1}{\sqrt{2+q^2}}(|\uparrow\downarrow\downarrow\rangle + q|\downarrow\uparrow\downarrow\rangle + |\downarrow\downarrow\uparrow\rangle), \\ e_0 &= \frac{J}{4}[J_2 - \Delta - \sqrt{(J_2 + \Delta - \Delta_2)^2 + 8}], \end{aligned}$$

where  $\Delta_2 = J_2\delta$ . In this notation  $|\uparrow\rangle, |\downarrow\rangle$  are the  $\sigma^z$  eigenbases, and

$$q = -\frac{1}{2}(J_2 + \Delta - \Delta_2 + \sqrt{(J_2 + \Delta - \Delta_2)^2 + 8}).$$

The interaction between blocks defines the effective interaction of the renormalised chain where each block is considered as a new single site. Calculating the effective Hamiltonian to the first order correction leads to the  $XXZ$  chain without next nearest neighbour interaction ( $J'_2 = 0$ ), i.e the effective Hamiltonian is not exactly similar to the initial one. The next-nearest neighbour interaction is the result of the second order correction. When the second order correction is added to the effective Hamiltonian, the renormalised Hamiltonian apart from an additive constant ( $e_B$ ) is similar to Eq.(1) with the renormalised couplings. Thus, the effective Hamiltonian including the second order correction is

$$\begin{aligned} H^{eff} = \frac{J'}{4} & \left[ \sum_i^{N/3} (\sigma_i^x \sigma_{i+1}^x + \sigma_i^y \sigma_{i+1}^y) + \Delta' (\sigma_i^z \sigma_{i+1}^z) \right. \\ & \left. + \sum_i^{N/3} J'_2 (\sigma_i^x \sigma_{i+2}^x + \sigma_i^y \sigma_{i+2}^y) + \Delta'_2 (\sigma_i^z \sigma_{i+2}^z) \right] + \frac{N}{3} e_B. \end{aligned}$$

The renormalised coupling constants are functions of the original ones which are given by the following equations.

$$\begin{aligned} J' &= J \left( \frac{2}{2+q^2} \right)^2 (q^2 + 2J_2q) - \frac{J^2}{4} \left( \frac{\Delta}{e_0 - e_2} \right) \left( \frac{q}{2+q^2} \right)^2 \\ &\quad - \frac{J^2}{4} \left( \frac{1}{e_0 - e_1} \right) \left( \frac{1}{(2+q^2)(2+p^2)} \right)^2 (p+q) \times \\ &\quad (pq)(p+q+4J_2)(\Delta - 2\Delta_2)pq + 4\Delta_2) \\ &\quad - \frac{J^2}{4} \left( \frac{4}{2e_0 - e_1 - e_2} \right) \left( \frac{1}{2+q^2} \right)^2 \left( \frac{q}{2+p^2} \right) \times \\ &\quad (p+q+2J_2)(\Delta - \Delta_2)pq + 2\Delta_2). \end{aligned} \tag{8}$$

$$\begin{aligned} \Delta' &= \left\{ J \left( \frac{q}{2+q^2} \right)^2 (\Delta q^2 + 2\Delta_2(2 - q^2)) \right. \\ &\quad - \frac{J^2}{4} \left( \frac{1}{e_0 - e_1} \right) \left( \frac{(p+q)^2 + 4J_2(p+q)}{(2+q^2)(2+p^2)} \right)^2 \\ &\quad - \frac{J^2}{4} \left( \frac{1}{e_0 - e_2} \right) \left( \frac{q^2}{2(2+q^2)} \right)^2 - \frac{J^2}{4} \left( \frac{1}{e_0 - e_3} \right) \left( \frac{1+2J_2q}{2+q^2} \right)^2 \\ &\quad - \frac{J^2}{4} \left( \frac{2}{2e_0 - e_1 - e_2} \right) \left( \frac{1}{2+p^2} \right) \left( \frac{q(p+q+2J_2)}{2+q^2} \right)^2 \\ &\quad + \frac{J^2}{4} \left( \frac{2}{2e_0 - e_2 - e_3} \right) \left( \frac{q(1+qJ_2)}{2+q^2} \right)^2 \\ &\quad \left. + \frac{J^2}{4} \left( \frac{4}{2e_0 - e_1 - e_3} \right) \left( \frac{J_2(pq+q^2+2)+p+q}{(2+q^2)(2+p^2)^{1/2}} \right)^2 \right\} / J'. \end{aligned} \tag{9}$$

$$J'_2 = \left\{ \frac{J^2}{4} \left( \frac{2}{2+q^2} \right)^3 \left[ \frac{J_2(3q+p) + q(p+q)^2}{(e_0 - e_1)(2+p^2)} + \frac{J_2(1+q^2) + q^2}{e_0 - e_3} - \frac{(q^2 + J_2q)^2}{2(e_0 - e_2)} \right] \right\} / J'. \quad (10)$$

$$\Delta'_2 = \left\{ \frac{J^2}{4} \left( \frac{2}{2+q^2} \right)^3 \left[ \frac{(\Delta_2q(p-pq^2+q) + \frac{\Delta}{2}pq^3)}{(e_0 - e_1)(2+p^2)} - \frac{(\Delta q^2 + \Delta_2(2-q^2))^2}{2(e_0 - e_2)} \right] \right\} / J'. \quad (11)$$

$$\begin{aligned} e_B &= \frac{1}{3}e_0 \\ &+ \frac{1}{3} \frac{J^2}{16} \left\{ \left( \frac{1}{e_0 - e_1} \right) \left( \frac{1}{(2+q^2)(2+p^2)} \right)^2 \left( (p+q)^2 + 4J_2(p+q) \right)^2 \right. \\ &+ \frac{1}{2} \left( pq(\Delta + 2\Delta_2(2-pq)) \right)^2 + \left( \frac{1}{e_0 - e_2} \right) \left( \frac{1}{2(2+q^2)} \right)^2 (q^2 + 8\Delta^2) \\ &+ \left( \frac{1}{e_0 - e_3} \right) \left( \frac{1+2J_2q}{2+q^2} \right)^2 + \left( \frac{2}{2e_0 - e_1 - e_2} \right) \left( \frac{1}{2+q^2} \right)^2 \left( \frac{1}{2+p^2} \right) \times \\ &\quad \left( ((p+q)q + 2J_2q)^2 + 2(\Delta pq + \Delta_2(2-pq))^2 \right) \\ &+ \left( \frac{4}{2e_0 - e_1 - e_3} \right) \left( \frac{1}{2+q^2} \right)^2 \left( \frac{1}{2+p^2} \right) \left( (p+q) + J_2q(p+q) + 2J_2 \right)^2 \\ &+ \left( \frac{2}{2e_0 - e_2 - e_3} \right) \left( \frac{q}{2+q^2} \right)^2 (1 + J_2q)^2 \left. \right\} \\ &+ \left( \frac{1}{3} \frac{J^2}{16} \right) \left\{ \left( \frac{2}{e_0 - e_3} \right) \left( \frac{2}{2+q^2} \right)^3 (q + J_2 + J_2q^2)^2 \right. \\ &+ \left( \frac{4}{e_0 - e_2} \right) \left( \frac{1}{2+q^2} \right)^3 (2(q^2 + J_2q)^2 + (\Delta q^2 + 2\Delta_2 - \Delta_2 q^2)^2) \\ &+ \left( \frac{2}{e_0 - e_1} \right) \left( \frac{1}{2+q^2} \right)^3 \left( \frac{1}{2+p^2} \right) \left( 8[q^2 + pq + 3J_2q + J_2p]^2 \right. \\ &\left. \left. + [pq(\Delta q^2 + 2\Delta_2 - \Delta_2 q^2) + \Delta_2 q^2(2-pq)]^2 \right) \right\}. \end{aligned} \quad (12)$$

in which

$$p = \frac{-1}{2} [J_2 + \Delta - \Delta_2 - \sqrt{(J_2 + \Delta - \Delta_2)^2 + 8}].$$

In the above equations,  $e_1, e_2$  and  $e_3$  are the first, second and third eigenenergies of the block's Hamiltonian which have analytic expressions in terms of the coupling constants but not presented here. Due to the level crossing which occurs for the eigenstates of the block Hamiltonian, RG equations are valid for  $\frac{1}{2}[(\Delta - \Delta_2) - \sqrt{(\Delta - \Delta_2)^2 + 4}] < J_2 < \frac{1}{2}[(\Delta - \Delta_2) + \sqrt{(\Delta - \Delta_2)^2 + 4}]$ . We have plotted the RG flow and different phases in Fig.(2) which will be discussed in the next section.

### III. PHASE DIAGRAM

The RG equations show the running of  $J$  coupling to zero which represents the renormalisation of energy scale. At the zero temperature, phase transition occurs upon variation of the parameters in the Hamiltonian. In the region of planar anisotropy  $0 \leq \Delta < 1$ , the nearest neighbour interaction ( $J_2 = 0$ ) is known not to support any kind of long range order and the ground state is the so called spin-fluid state. Increasing the amount of anisotropy is necessary to

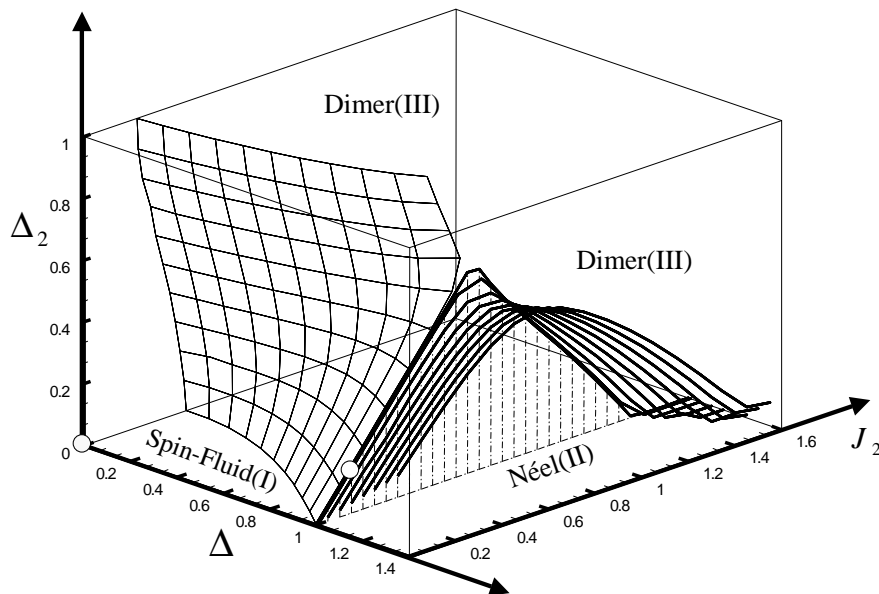


FIG. 2: Phase diagram of the XXZ model with next-nearest neighbour interaction and different anisotropies. Open circles show the fixed points, the tri-critical point ( $\Delta_2^* = J_2^* \simeq 0.155, \Delta^* = 1$ ) and the XY fixed point ( $\Delta_2^* = J_2^* = \Delta^* = 0$ ). For  $0 \leq \Delta \leq 1$ , the front side of diagram is the spin-fluid phase (I) and the back side is the dimer phase (III). The checkerboard pattern represents the boundary between them. In the case of  $\Delta > 1$  there are two phases, the Néel-phase (II) which exists below the semi-circular lines and the dimer-phase (III) which is above them. The boundary between Néel and dimer phases is shown by the semi-circular lines. The surface which is depicted by the dash-dotted lines is the boundary between the dimer-Néel phases which is a vertical plane at  $\Delta = 1$ . The phase transition between the spin-fluid phase (I) and the dimer phase (III) occurs at the vertical plane  $\Delta = 1$  which has not been plotted in this diagram to avoid it being complex.

stabilize the spin alignment. For  $\Delta > 1$  the ground state is the Néel ordered state. In the case of  $J_2 > 0$ , the nearest neighbour and next-nearest neighbour couplings are in competition with each other. The latter thus frustrates the ordering tendency of the former. For  $0 \leq \Delta < 1$  the interplay of the two competing terms in the presence of quantum fluctuations produces the dimer phase for  $J_2 \geq J_2^c(\Delta, \Delta_2)$ . Our RG equations show that the phase boundary between the dimer and the spin-fluid phase depends on the n-n-n anisotropy coupling ( $\Delta_2$ ) and can be described by a two dimensional surface which is convex in a view from the spin-fluid phase (see Fig.(2), the checkerboard curved plane).

The dimer or spin Peierls phase has a spin gap and a broken translation symmetry (the unit cell is doubled) in the thermodynamic limit. The dimer-fluid transition is known to be of Berzinskii-Kosterlitz-Thouless (BKT) type [29]. At the BKT transition point, the divergence of the correlation length is not of the usual power law type but very singular [30]. In fact, all the derivatives of the inverse of the correlation length at the critical point are zero. Moreover, at the BKT critical point there appear the logarithmic correction as a finite size effect which converges very slowly, in various quantities, such as correlation function and susceptibilities, therefore it is very difficult to find the critical point of the BKT type transition accurately. Two effective methods have been introduced to find this critical point. In the work of Roomany et. al [31],  $\beta$ -function is calculated numerically, while in the Nomura-Okamoto approach [9] the fluid-dimer transition is determined by the degeneracy between the doublet excitation and the dimer excitation. Moreover, in Ref.[26] a proper structure factor has been introduced to probe this transition. However, we determine the fluid-dimer phase transition by using the running of couplings under RG. In the spin-fluid phase, the anisotropy and next-nearest neighbour couplings are irrelevant while in the dimer phase they run to the tri-critical point ( $\Delta_2^* = J_2^* \simeq 0.155, \Delta^* = 1$ ). For small  $\Delta_2$  the fluid-dimer phase boundary ( $J_2^c(\Delta)$ ) shows an inclination to the lower values versus  $\Delta$  while it behaves conversely for higher  $\Delta_2$  as shown in Fig.(2). The comparison with numerical results [9] for  $\Delta = \delta$  shows good qualitative agreement. The projection of the three dimensional phase diagram (Fig.(2)) on the  $\Delta_2 = J_2\Delta$  plane is shown in Fig.(3). Different phases and the running of RG flows can be observed simply. However, from quantitative point of view we got higher values for  $J_2^c$  than the numerical results. For instance,

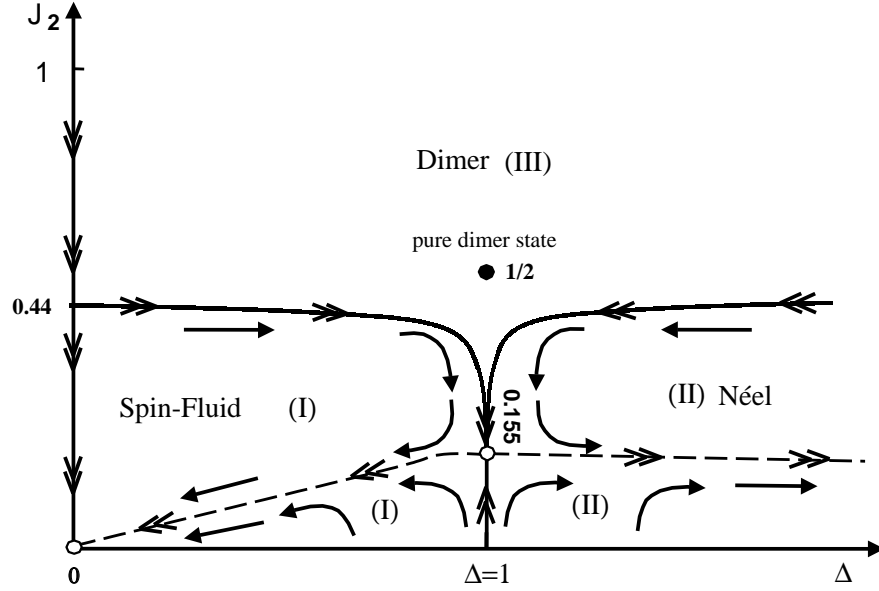


FIG. 3: The projection of the 3-dimensional phase diagram (Fig.(2)) on the  $\Delta_2 = J_2\Delta$  plane. Arrows show the running of couplings under RG. Open circles show fixed points. The dashed lines in the spin-fluid and Néel phases are the lines of the Gaussian fixed point. Different phases are labeled by: (I) spin-fluid, (II) Néel order, (III) dimer. The Filled circle denoted by  $J_2 = 1/2$  on the  $\Delta = 1$  line is the pure dimer state.

at  $\Delta = 0$  the RG analysis gives  $J_2^c \simeq 0.44$  which can be compared with the numerical result of  $J_2^c \simeq 0.33$  presented in Ref.[9]. The difference is inherited to the QRG scheme where the boundary condition of the isolated block does not represent the presence of the rest of chain [32, 33].

In the region of the antiferromagnetic anisotropy ( $\Delta > 1$ ) where the Néel phase exists, it is destabilized by sufficiently strong competing next-nearest neighbour couplings,  $J_2^c$  and  $\Delta_2^c$ . The Néel phase appears just by crossing the  $\Delta = 1$  plane at  $\Delta_2 = 0$  and  $J_2 = 0$ . In the  $\Delta_2 = 0$  plane and for  $\Delta > 1$  the model will pass through a phase transition from Néel to dimer phase for  $J_2 > J_2^c(\Delta)$ . This boundary is the intersection of the semi-circular lines and the  $\Delta_2 = 0$  plane which happens around  $J_2 \sim 1.5$  (see Fig.(2)). The Néel ordered is also broken by increasing the anisotropy of the n-n-n interaction. This is a phase transition to the dimer phase which is shown in Fig.(2) by the semi-circular lines where the dimer phase exists above them. Thus, both the n-n-n exchange ( $J_2$ ) and n-n-n anisotropy ( $\Delta_2$ ) drive the model from the Néel ordered phase to the dimer one. In this respect, the boundary between the Néel and the dimer phase looks like an arcade in the phase diagram.

We have probed the boundary of the Néel-dimer transition by calculating the staggered magnetisation in the  $z$ -direction as an order parameter (Fig.(4)),

$$S_M = \frac{1}{N} \sum_{i=1}^N (-1)^i \langle \sigma_i^z \rangle. \quad (13)$$

The staggered magnetisation ( $S_M$ ) is zero in the dimer phase and has a nonzero value in the Néel phase. Thus the staggered magnetisation is the proper order parameter to represent the Néel-dimer transition. We have plotted  $S_M$  versus  $\Delta_2$  for different values of  $\Delta = 1.05, 1.15$  and  $J_2 = 0.3, 0.6$  in Fig.(4). The staggered magnetization goes to zero continuously at a critical value of  $\Delta_2^c(\Delta, J_2)$  which shows the destruction of Néel order.

A similar calculation has been done to trace the phase transition between the Néel and the spin-fluid phase. The crossing boundary of the fluid and Néel phases always stays at  $\Delta = 1$ . The reason is related to the  $SU(2)$  symmetry of the Hamiltonian on the line  $\Delta = \delta = 1$ . The QRG approach preserves this symmetry which can be seen by the irrelevant direction of  $\Delta_2 = J_2$  in the  $\Delta = 1$  plane toward the tri-critical point.

The significant result of our calculations occurs at the isotropic plane,  $\Delta = 1$ . For small  $J_2$  the RG equations show running of  $J_2$  to zero except at the isotropic plane ( $\Delta = 1$ ). This means, if we start with the XXX model ( $J_2 = 0$ ), the next-nearest neighbour interaction ( $J_2$ ) is generated and runs to the tri-critical point,  $\Delta_2^* = J_2^* = 0.155$ ,  $\Delta^* = 1$ . It might be interesting to mention that this fixed point corresponds to the reported experimental value for  $CuGeO_3$  ( $J_2 = 0.13$ ) [13]. It is worth mentioning that for the isotropic case  $\Delta = \delta = 1$ , if the projection operator for the

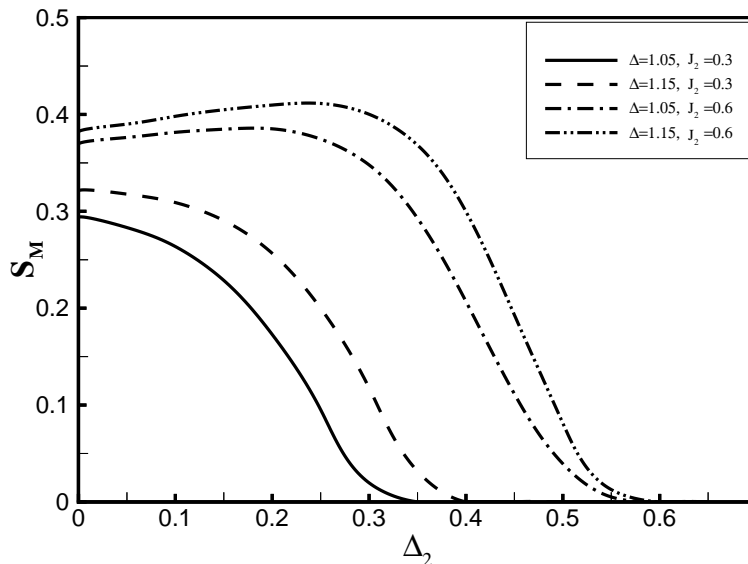


FIG. 4: The staggered Magnetisation in z-direction for different values of  $\Delta$  and  $J_2$  versus  $\Delta_2$ . The order parameter ( $S_M$ ) goes continuously to zero which represents the transition from Néel to dimer phase.

second order RG,  $(1 - P_0)$ , does not contain all of the remaining states of the block we get  $J_2^* = 0.0761$  [28]. This shows the increase of  $J_2^*$  when we have considered the correlation effects more precisely. Thus, we expect a nonzero value for  $J_2^*$  if we go further to consider the higher order RG approximation. This is also true for  $J_2 = 0$  as the initial value, the corresponding fixed point is nonzero. So, the manageable fixed point, the fixed point which enables us to get the physical quantity, represents the next-nearest neighbour interaction for the isotropic Heisenberg chain. At this fixed point the correlation length is zero and the system behaves as a classical one. It represents a frustrated chain of classical spins which does not possess any ordering. It might be an explanation why the nearest neighbour one-dimensional antiferromagnetic Heisenberg chain does not show a true long range order.

The other remarkable result of our RG flow is the observation of the specific lines in the spin-fluid and Néel phases which has been shown by dashed lines in Fig.(3). We have linearised the RG flow at  $(\Delta_2^* = J_2^* \simeq 0.155, \Delta^* = 1)$ , and found one relevant and two irrelevant directions. The eigenvalues of the matrix of linearised flow are  $\lambda_1 = 1.24$ ,  $\lambda_2 = 0.46$  and  $\lambda_3 = 0.41$ . The corresponding eigenvectors in the  $|\Delta, J_2, \Delta_2\rangle$  coordinates are  $|\lambda_1\rangle = |-0.98, 0.02, -0.20\rangle$ ,  $|\lambda_2\rangle = |-0.88, 0.15, -0.44\rangle$  and  $|\lambda_3\rangle = |0, 0.707, 0.707\rangle$ . The direction of the dashed lines in Fig.(3) close to the tri-critical point corresponds to  $|\lambda_1\rangle$ . The two dashed lines start at  $\Delta^* = 1, J_2^*$ , one of them ends at the XY fixed point ( $\Delta = 0, J_2 = 0$ ) and the other ends in the Ising fixed point ( $\Delta = \infty, J_2 = 0$ ). Although these lines separate two different RG flows below and above the dash lines the flows represent a unique phase which is the spin-fluid for  $\Delta < 1$  and the Néel phase for  $\Delta > 1$ . These lines are supposed to be the Gaussian fixed points which have been reported in Ref.[9]. In the spin-fluid and Néel phases, large distance physics is described by the Gaussian model where the system possesses the conformal symmetry [34].

We have also calculated some critical exponents at the tri-critical point. In this respect, we have obtained the dynamical exponent, the exponent of order parameter and the diverging exponent of the correlation length. This corresponds to reaching the tri-critical point from the Néel phase by approaching  $\Delta \rightarrow 1$ . The scaling of gap exponent is  $z \simeq 0.83$ , the staggered magnetization goes to zero like  $S_M \sim |\Delta - 1|^\beta$  with  $\beta \simeq 0.82$  and the correlation length diverges at  $\Delta = 1$  with exponent  $\nu \simeq 2.27$ . The detail of a similar calculation can be found in Ref.[5].



TABLE I: The first ( $e_{BRG}^{(1)} = \frac{E_{BRG}^{(1)}}{JN}$ ) and second ( $e_{BRG}^{(2)} = \frac{E_{BRG}^{(2)}}{JN}$ ) order approximations of the ground state energy per site are compared with the exact ( $e^{exact} = \frac{E^{exact}}{JN}$ ) value [14]. The relative errors,  $\epsilon^{(1)} = \frac{E_{BRG}^{(1)} - E^{exact}}{E^{exact}}$  and  $\epsilon^{(2)} = \frac{E_{BRG}^{(2)} - E^{exact}}{E^{exact}}$  have also been shown.

$\Delta$	$e^{exact}$	$e_{BRG}^{(1)}$	$e_{BRG}^{(2)}$	$\epsilon^{(1)}$	$\epsilon^{(2)}$
0.0	-0.3183	-0.2828	-0.3229	11.1%	2.3%
0.1	-0.3286	-0.2921	-0.3319	11.1%	1%
0.2	-0.3395	-0.3016	-0.3390	11.1%	0.14%
0.3	-0.3509	-0.3115	-0.3470	11.2%	1.1%
0.4	-0.3627	-0.3217	-0.3559	11.3%	1.8%
0.5	-0.3750	-0.3322	-0.3656	11.4%	2.5%
0.6	-0.3877	-0.3432	-0.3759	11.4%	3.04%
0.7	-0.4009	-0.3545	-0.3870	11.5%	3.4%
0.8	-0.4145	-0.3663	-0.3988	11.6%	3.7%
0.9	-0.4286	-0.3785	-0.4112	11.6%	4.05%

#### IV. SUMMARY AND DISCUSSIONS

We have presented the second order RG approximation to obtain the phase diagram, staggered magnetisation and ground state energy of the XXZ chain with next-nearest neighbour interaction. We have observed that the second order RG equations must be considered to get a self similar Hamiltonian upon renormalisation processes. The ground state energy density of the nearest neighbour  $XXZ$  ( $J_2 = 0$ ) model in the limit  $N \rightarrow \infty$  is then given by,  $e_{\infty}^{BRG} = \sum_{m=0}^{\infty} \frac{1}{3^{m+1}} e_B(J^{(m)}, \Delta^{(m)})$  where initially  $J^{(0)} = J$  and  $\Delta^{(0)} = \Delta$ . We have considered the nearest neighbour case to be able to compare with the exact results. We have shown this quantity in Table.(1) where the results of the first and second order RG presented for  $0 \leq \Delta < 0.9$ . The relative error has been derived by comparison with the exact result [14]. The second order correction improves the relative error at least to 65 percent. However the improvement of the 2nd order approximation is not monotonic for the whole range of  $\Delta$ .

An interesting result of the QRG scheme is the case of isotropic Heisenberg model ( $J_2 = 0, \Delta = 1$ ) which runs to the frustrated next-nearest neighbour fixed point under the second order RG equations. This can be viewed as an explanation for the absence of long range order in the nearest neighbour antiferromagnetic Heisenberg model. Moreover, our primary calculation to take into account the higher order RG equations shows that the effective (renormalised) Hamiltonian will consist of the long range interactions. Taking into account the third order correction will result in an infinite range interaction of XXZ type. We would also like to mention a comment on the implementation of the 2nd order RG approach. The calculation is straightforward (not necessarily simple) whenever the zeroth order projection operator ( $P_0$ ) is composed of degenerate states. This makes possible to obtain the effective Hamiltonian in the analytic form. We have tried to get the 2nd order corrections for the  $S = \frac{1}{2}$  XYZ model in the transverse field where the block ground-state is not degenerate. We were not able to obtain the analytic 2nd order corrections. This is important because the advantage of the QRG is the analytic form of results which helps to get the phase diagram even though it may not be quantitatively very accurate. If we are forced to do the RG approach in a numerical way then it is appropriate to implement the Density Matrix Renormalisation Group (DMRG) method. In that case, we loose the renormalisation group features of the running of the coupling constants but get the accurate numerical values.

#### V. ACKNOWLEDGMENT

The authors would like to thank P. Thalmeier for reading the manuscript and his comments.

## References

- 
- [1] M. Vojta, Rep. Prog. Phys. **66**, 2069 (2003) and references therein
  - [2] K. G. Wilson, Rev. Mod. Phys. **47**, 773 (1975).
  - [3] S. D. Drell, M. Weinstein, and S. Yankielowicz, Phys. Rev. D **14**, 487 (1979).
  - [4] A. L. Stella, C. Vanderzand, and R. Dekeyser, Phys. Rev. B **27**, 1812 (1983).
  - [5] M. A. Martin-Delgado and G. Sierra, Int. J. Mod. Phys. A **11**, 3145 (1996).
  - [6] A. Drzewinski and J. M. J. Van Leeuwen, Phys. Rev. B **49**, 403 (1994).
  - [7] A. Langari, Phys. Lett. A **246**, 359 (1998); A. Langari, Phys. Rev. B **58**, 14467 (1998).
  - [8] A. Langari, Phys. Rev. B **69**, 100402(R) (2004)
  - [9] K. Nomura and K. Okamoto, J. Phys. A **27**, 5773 (1994).
  - [10] M. Hase, I. Terasaki, and K. Uchinokura, Phys. Rev. Lett. **70**, 3651 (1993).
  - [11] N. Motoyama, H. Eisaki and S. Uchida, Phys. Rev. Lett. **76**, 3212 (1996).
  - [12] R. Coldea, D. A. Tennant, R. A. Cowley, D. F. McMorrow, B. Dorner, and Z. Tylczynski, Phys. Rev. Lett. **79**, 151 (1997).
  - [13] Y. Mizuno, T. Tohyama, S. Maekawa, T. Osafune, N. Motoyama, H. Eisaki, and S. Uchida, Phys. Rev. B **57**, 5326 (1998).
  - [14] J. des Cloizeaux and M. Gaudin, J. Math. Phys. **7**, 1384 (1966).
  - [15] C. N. Yang and C. P. Yang, Phys. Rev. **151**, 258 (1966).
  - [16] C. K. Majumdar and D. K. Ghosh, J. Math. Phys. **10**, 1399 (1969); C. K. Majumdar and D. K. Ghosh, J. Phys. C: Solid State Phys. **3**, 911 (1970).
  - [17] F. D. M. Haldane, Phys. Rev. B **25**, 4925 (1982); (erratum Phys. Rev. B **26**, 5257 (1982)).
  - [18] T. Tonegawa and I. Harada, J. Phys. Soc. Japan **56**, 2153 (1987); T. Tonegawa and I. Harada, Proc. Int. Conf. on Magnetism; J. Physique Coll. Suppl. **49**, C8 1411 (1988).
  - [19] J. Igarashi and T. Tonegawa, Phys. Rev. B **40**, 756 (1989); J. Igarashi and T. Tonegawa J. Phys. Soc. Japan. **58**, 2147 (1989).
  - [20] K. Kuboki and H. Fukuyama, J. Phys. Soc. Japan. **56**, 3126 (1987).
  - [21] I. Affleck, D. Gepner, H. J. Schulz and T. Ziman, J. Phys. A: Math. Gen. **22**, 511 (1989).
  - [22] T. Tonegawa, I. Harada, and J. Igarashi, Prog. Theor. Phys. Suppl. **101**, 513 (1990).
  - [23] T. Tonegawa, I. Harada, and M. Kaburagi, J. Phys. Soc. Japan **61**, 4665 (1992).
  - [24] K. Okamoto and K. Nomura, Phys. Lett. A. **169**, 433 (1992).
  - [25] S. Eggert, Phys. Rev. B **54**, 9612 (1996).
  - [26] C. Gerhardt, A. Fledderjohan, E. Aysal, K-H. Muetter, J. F. Audet, and H. Kröger J. Phys.: Condens. Matter **9**, 3435 (1997).
  - [27] G. Sierra and M. A. Martin Delgado, in *Strongly Correlated Magnetic and Superconducting Systems*, Lecture Notes in Physics Vol. 478 (Springer, Berlin, 1997).
  - [28] M. A. Martin-Delgado, *Proceedings of the El Escorial Summer School on Strongly Correlated Magnetic and Superconducting Systems, 1996, cond-mat/9610196*
  - [29] V. L. Berzinskii, Zh. Eksp. Teor. Fiz. **59**, 907 (1970) [Sov. Phys. JETP **32**, 493 (1970).]; J. M. Kosterlitz, *ibid* **7**, 1046 (1974).
  - [30] J. M. Kosterlitz and D. J. Thouless, J. Phys. C **6**, 1181 (1973).
  - [31] H. H. Rommany and H. W. Wyld, Phys. Rev. D **23**, 1357 (1981); H. H. Rommany and H. W. Wyld Phys. Rev. D **21**, 3341 (1980).
  - [32] S. R. White and R. M. Noack, Phys. Rev. Lett. **68** 3487 (1992).
  - [33] M. A. Martin-Delgado and G. Sierra, Phys. Lett. B **364**, 41 (1995).
  - [34] P. Di Francesco, P. Mathieu, and D. Senechal, *Conformal Field Theory* (Springer-Verlag, New York, 1997).